

# The Effect of Alkane Structure on Rates of Photoinduced C–H Bond Activation by Cp\*Rh(CO)<sub>2</sub> in Liquid Rare Gas Media: An Infrared Flash Kinetics Study

Bruce K. McNamara, Jake S. Yeston, Robert G. Bergman,<sup>\*,†</sup> and C. Bradley Moore<sup>\*,†</sup>

Contribution from the Department of Chemistry, University of California, Berkeley, California 94720-1460, and Chemical Sciences Division, Lawrence Berkeley National Laboratory, Berkeley, California 94720-1460

Received February 10, 1999

**Abstract:** C–H bond activation via photoinduced reaction of Cp\*Rh(CO)<sub>2</sub> (**1**) with alkanes (RH) in liquid Kr and liquid Xe solution has been studied by time-resolved infrared spectroscopy. Irradiation leads to the formation of a transient species absorbing at 1947 cm<sup>-1</sup> in liquid Kr. Reaction rates for the conversion of this species to the final C–H activation product Cp\*(CO)Rh(R)(H) (**4**) have been measured in the –80 to –110 °C temperature range for a series of linear and cyclic alkanes. No reaction was observed with methane; for all other hydrocarbons, the dependence of the reaction rate on the alkane concentration follows saturation kinetics. Analysis of the kinetic data was carried out using the assumption, established in earlier work, that the observed transient is a mixture of two solvates, a krypton complex Cp\*Rh(CO)•Kr (**2**) and an alkane complex Cp\*Rh(CO)•RH (**3**), both having essentially the same CO stretching frequency in the IR. For each alkane, the rate law supports a deconvolution of the overall reaction into an alkane binding step and an oxidative addition step. For the binding step, the parameter *K*<sub>eq</sub> and its associated free energy characterize a preequilibrium between **2** and **3**. Within each series (linear and cyclic), as alkane size increases, the measured free energy of binding of the alkane to the coordinatively unsaturated Rh center in the Cp\*Rh(CO) fragment becomes increasingly thermodynamically favorable, ranging from –0.9 (ethane) to –2.3 kcal/mol (octane) and from –2.4 (cyclopentane) to –3.5 kcal/mol (cyclooctane) at –90 °C relative to Kr. The second step, oxidative addition of the C–H bond across the Rh center to convert **3** to **4**, proceeds with an absolute rate characterized by the parameter *k*<sub>2</sub>. This rate exhibits very little variance in the series of linear alkanes. Propane, hexane, and octane each react with a rate constant of roughly (6–7) × 10<sup>5</sup> s<sup>-1</sup> at –90 °C, while ethane reacts about a factor of 3 more rapidly. More variance is observed in the cyclic series. Oxidative addition of cyclopentane proceeds with a rate constant of 6.8 × 10<sup>5</sup> s<sup>-1</sup> at –90 °C, while the oxidative addition rates of cycloheptane and cyclooctane are slower by an order of magnitude. Possible explanations are discussed for this unexpected alkane structure dependence in both steps of the reaction.

## Introduction

It has been more than fifteen years since Bergman and Graham independently characterized the first examples of aliphatic C–H bond oxidative addition by soluble organometallic complexes.<sup>1,2</sup> In the intervening time, quite a number of organotransition metal complexes have been shown to undergo this reaction with simple alkanes.<sup>3–5</sup> The transformation has intrigued researchers both because of its industrial potential as a means of selectively functionalizing hydrocarbons and because of the remarkable facility with which unsaturated metal centers can cleave such strong bonds. There have thus been a great number of kinetic, mechanistic, and theoretical studies focused on aliphatic C–H activation, carried out by our own group and others.<sup>6–16</sup>

The structural and kinetic features of the metal–alkane interaction prior to oxidative addition remain an area of active

inquiry. Both theoretical and experimental work suggests that alkanes coordinate to metals with significant binding energies (often ca. 5–12 kcal/mol), and that the transition metal alkane complexes (sometimes referred to as solvates or “σ-complexes”) thus formed are discrete intermediates in C–H activation.<sup>6,10,17–20</sup> These results establish that the ratios of C–H activation products formed in traditional competition studies, in which a reactive

(5) Arndtsen, B. A.; Bergman, R. G.; Mobley, T. A.; Peterson, T. H. *Acc. Chem. Res.* **1995**, *28*, 154.

(6) Mobley, T. A.; Schade, C.; Bergman, R. G. *Organometallics* **1998**, *17*, 3574.

(7) Bromberg, S. E.; Yang, H.; Asplund, M. C.; Lian, T.; McNamara, B. K.; Kotz, K. T.; Yeston, J. S.; Wilkens, M.; Frei, H.; Bergman, R. G.; Harris, C. B. *Science* **1997**, *278*, 260.

(8) Bennett, J. L.; Wolczanski, P. T. *J. Am. Chem. Soc.* **1997**, *119*, 10696.  
(9) Osman, R.; Pattison, D. I.; Perutz, R. N.; Bianchini, C.; Casares, J. A.; Peruzzini, M. *J. Am. Chem. Soc.* **1997**, *119*, 8459.

(10) Stahl, S. S.; Labinger, J. A.; Bercaw, J. E. *J. Am. Chem. Soc.* **1996**, *118*, 5961.

(11) Jones, W. D.; Hessel, E. T. *J. Am. Chem. Soc.* **1993**, *115*, 554.

(12) For recent theoretical studies, see the following, as well as refs 13–16: Su, M. D.; Chu, S. Y. *Chem. Eur. J.* **1999**, *5*, 198.

(13) Su, M. D.; Chu, S. Y. *J. Phys. Chem. A* **1997**, *101*, 6798.

(14) Zaric, S.; Hall, M. B. *J. Phys. Chem. A* **1998**, *102*, 1963.

(15) Wittborn, A. M. C.; Costas, M.; Blomberg, M. R. A.; Siegbahn, P. E. M. *J. Chem. Phys.* **1997**, *107*, 4318.

(16) Siegbahn, P. E. M. *J. Am. Chem. Soc.* **1996**, *118*, 1487.

<sup>†</sup> Address correspondence to either of these authors at the University of California.

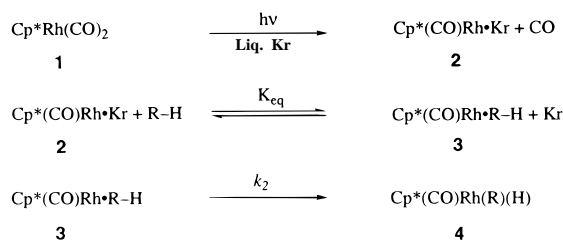
(1) Janowicz, A. H.; Bergman, R. G. *J. Am. Chem. Soc.* **1982**, *104*, 352.

(2) Hoyano, J. K.; Graham, W. A. G. *J. Am. Chem. Soc.* **1982**, *104*, 3723.

(3) Stahl, S. S.; Labinger, J. A.; Bercaw, J. E. *Angew. Chem., Int. Ed. Engl.* **1998**, *37*, 2181.

(4) Shilov, A. E.; Shulpin, G. B. *Chem. Rev.* **1997**, *97*, 2879.

## Scheme 1



metal complex is allowed to react in a mixture of two or more alkanes, cannot be interpreted as a simple function of two competing C–H activation steps. Rather, the final products are determined both by the binding of each alkane to the metal center and by the relative rates of the elementary C–H bond insertion steps. Time-resolved studies in neat alkane solvent rarely permit a meaningful comparison of alkane binding affinities, since under these conditions the binding step typically occurs on a picosecond or subpicosecond time scale.<sup>21</sup> Studies in rare gas media, however, have presented a unique opportunity to examine alkane binding affinities independently, and thus to assess their role in controlling C–H activation selectivities.

The work reported here concerns C–H activation achieved by photoinduced reaction of  $\text{Cp}^*\text{Rh}(\text{CO})_2$  (**1**) with alkanes in liquid krypton or xenon solution. The reaction proceeds on a microsecond time scale at low temperature and has been studied in our group previously by infrared flash kinetic spectroscopy. These early studies employed cyclohexane, neopentane, and their perdeuterated analogues as substrates.<sup>22,23</sup> The results supported the mechanism shown in Scheme 1. Photolysis induces CO loss from the parent complex to form a krypton-solvated rhodium species **2**. Solvation by the rare gas sequesters the complex until the less inert alkane enters the coordination sphere of the metal. The data are most consistent with a well-defined preequilibrium between discrete Rh–Kr (**2**) and Rh–alkane (**3**) solvates. The alkane solvate **3** then reacts thermally by oxidative addition of a C–H bond across the rhodium center to form a rhodium alkyl hydride product (**4**).<sup>24</sup>

The mechanism outlined in Scheme 1 can be analyzed according to a modified Michaelis–Menten model, assuming rapid preequilibrium, to give the expression shown in eq 1 for

$$k_{\text{obs}} = \frac{k_2[\text{R-H}]}{[\text{R-H}] + \frac{[\text{Kr}]}{K_{\text{eq}}}} \quad (1)$$

$k_{\text{obs}}$ , the pseudo-first-order rate constant measured under flooding conditions in alkane (large excess relative to Rh).<sup>23,25</sup> A derivation of the expression is given in the Supporting Information. By fitting the rate data to this expression at various alkane concentrations, it is possible to extract two specific param-

eters:  $K_{\text{eq}}$ , which characterizes the extent to which the preequilibrium favors the alkane complex over the rare gas complex in the preequilibrium, and  $k_2$ , which represents the elementary rate constant for the oxidative addition step from the alkane complex. Thus direct and separate comparisons can be made between the binding affinities of various alkanes for the Rh center, and between the rates of elementary C–H bond insertion.

A comparison of the parameters for reaction of **1** with cyclohexane and with neopentane indicated a definite impact of alkane structure on both the binding step and the oxidative addition step. A better understanding of this impact is of particular interest in characterizing and predicting selectivities in C–H activation reactions. To this end, we have employed infrared flash kinetic spectroscopy for systematic rate measurements of the photolytic reaction of **1** with a series of linear and cyclic alkanes in liquid rare gas solution.

## Experimental Section

The apparatus and techniques employed for flash infrared kinetic studies in our laboratories have been described in detail previously.<sup>23</sup> Briefly, reactions were performed in a high-pressure, temperature-controlled copper cell. Kinetics were measured using a standard pump-probe scheme, with the reaction initiated by a 308 nm pulse from a XeCl excimer laser (Lambda Physik EMG 103 or Compaq 102) and probed using the tunable output of an IR diode laser (Mütek model MDS 2020) impinging on a liquid-N<sub>2</sub>-cooled InSb detector (Cincinnati Electronics model SDD-32E0-S1, 100 ns rise time). Reaction mixtures were also characterized using a Nicolet 550 FTIR spectrometer.

Krypton and xenon (99.999%) were purchased from Spectra Gases and used as received. Ethane, propane, and butane (all 99.999%) were purchased from Matheson and used as received. Liquid alkanes (all 99% or greater) were purchased from Aldrich or Acros, stirred over H<sub>2</sub>SO<sub>4</sub> and H<sub>2</sub>SO<sub>4</sub>/permanganate solutions to remove olefinic impurities, dried successively over sodium sulfate and either calcium hydride or elemental sodium, and vacuum transferred immediately before use.  $\text{Cp}^*\text{Rh}(\text{CO})_2$  (**1**) was either prepared according to a literature procedure<sup>26</sup> or purchased from Strem Chemicals.

The concentration of **1** employed in each kinetic run was roughly  $10^{-4}$  M. Alkane concentrations were determined by integration of appropriate bands in FTIR spectra of the reaction mixture acquired at each temperature at which kinetic measurements were taken. Integrated molar absorption coefficients at several wavelengths for the lower boiling hydrocarbons ethane and propane were calculated from Beer's law plots constructed by condensing known liquid volumes of the alkane into the high-pressure cell. The alkane was frozen in the cell at  $-150$  °C and the cell evacuated, after which Kr was condensed into the cell at  $-110$  °C. The liquid krypton solution was equilibrated at  $-80$  °C until no change in the infrared absorbance of the hydrocarbon bands was observed. Absorption coefficient data, corrected for index of refraction, matched gas-phase literature values to within 10% at  $-110$  °C.<sup>27</sup> It was found for the heavier liquid hydrocarbons that introduction of precise small quantities of alkane into the cell was very difficult, and that greater accuracy in determining absorption coefficients could be achieved using Beer's law plots constructed from standard solutions of the alkane prepared in carbon tetrachloride. IR spectra of these standard solutions were acquired at room temperature using a 0.1 cm path length cell. These spectra matched those of the hydrocarbons in liquid Kr, with the exception of 2 to 5  $\text{cm}^{-1}$  peak shifts, as well as narrowing of the hydrocarbon absorption bandwidths in Kr (typical

(24) For three out of the four alkane substrates studied, the krypton and alkane solvates were believed to exhibit overlapping CO stretching bands at  $1947$   $\text{cm}^{-1}$ . Crucial support for this hypothesis was obtained by study of the reaction of **1** with perdeuterioisopentane, which permitted spectroscopic and temporal resolution of IR bands at  $1946$  and  $1947$   $\text{cm}^{-1}$ , attributable to the putative krypton and alkane complexes, respectively. See ref 22.

(25) Weiller, B. H.; Wasserman, E. P.; Bergman, R. G.; Moore, C. B.; Pimentel, G. C. *J. Am. Chem. Soc.* **1989**, *111*, 8288.

(26) Kang, J. W.; Maitlis, P. M. *J. Organomet. Chem.* **1971**, *26*, 393.

(27) Kondo, S.; Saeki, S. *Spectrochim. Acta* **1973**, *29A*, 735.

(17) Gross, C. L.; Girolami, G. S. *J. Am. Chem. Soc.* **1998**, *120*, 6605.

(18) Schafer, D. F.; Wolczanski, P. T. *J. Am. Chem. Soc.* **1998**, *120*, 4881.

(19) For a recent review of experimental and theoretical work on transition metal alkane complexes, see: Hall, C.; Perutz, R. N. *Chem. Rev.* **1996**, *96*, 3125.

(20) A complex between cyclopentane and a photogenerated  $\text{CpRe}(\text{CO})_2$  fragment has recently been characterized by low-temperature <sup>1</sup>H NMR spectroscopy: Gefitakis, S.; Ball, G. E. *J. Am. Chem. Soc.* **1998**, *120*, 9953.

(21) Bromberg, S. E.; Lian, T. Q.; Bergman, R. G.; Harris, C. B. *J. Am. Chem. Soc.* **1996**, *118*, 2069.

(22) Bengali, A. A.; Schultz, R. H.; Moore, C. B.; Bergman, R. G. *J. Am. Chem. Soc.* **1994**, *116*, 9585.

(23) Schultz, R. H.; Bengali, A. A.; Tauber, M. J.; Weiller, B. H.; Wasserman, E. P.; Kyle, K. R.; Moore, C. B.; Bergman, R. G. *J. Am. Chem. Soc.* **1994**, *116*, 7369.

**Table 1.** IR Bands Assigned to Cp\*Rh(CO)(alkyl)(H) in Liquid Kr

alkane	$\nu_{\text{CO}}$ (cm <sup>-1</sup> )	alkane	$\nu_{\text{CO}}$ (cm <sup>-1</sup> )
ethane	2007(±2)	cyclopentane	2005(±2)
propane	2005(±2)	cyclohexane <sup>a</sup>	2003(±2)
hexane	2007(±2)	cycloheptane	2004(±2)
octane	2005(±2)	cyclooctane	2000(±2)

<sup>a</sup> Reference 23.

fwhm values were 3–4 cm<sup>-1</sup> in Kr and 7–8 cm<sup>-1</sup> in CCl<sub>4</sub>). Beer's law data obtained by dissolution of known amounts of cyclohexane in liquid Kr confirmed the accuracy of the absorption coefficients obtained in CCl<sub>4</sub> to within 10%.

In typical kinetic runs, as the cell temperature was raised from –110 to –80 °C, the vapor pressure of the liquid krypton solution increased from 200 to 800 psi. The liquid volume visibly increased as well. These changes in experimental conditions were observed to cause a systematic change in the hydrocarbon absorption intensities. Specifically, lowering the solution temperature from –80 to –110 °C gave rise to a 20% increase in integrated absorption intensity.<sup>28</sup> Kr/hydrocarbon vapor pressure data suggest that between –80 and –110 °C less than 2% of the dissolved alkane evaporates into the headspace of the cell, even in the case of ethane.<sup>29,30</sup> Variable-temperature <sup>1</sup>H NMR experiments using Kr/ethane solutions in a high-pressure NMR tube have confirmed this estimation. We therefore attribute the changes in band intensity to actual changes in hydrocarbon concentration. These result from a decrease in the density of the liquid Kr with rising temperature and consequent increase in the overall solution volume.<sup>31</sup> Alkane concentrations were therefore evaluated independently at each temperature of interest.

## Results

**Photolysis of 1 in Liquid Krypton/Alkane Solutions.** As shown by previous work in our group, photolysis of **1** in pure liquid krypton results in detector-limited rise of a transient absorption at 1947 cm<sup>-1</sup>. This species exhibits well-defined, single-exponential decay behavior over a 200 μs interval at –80 °C and has been assigned to Kr solvate **2**, Cp\*Rh(CO)•Kr.<sup>23</sup> In the presence of alkane, the observed rate constant for decay of the 1947 cm<sup>-1</sup> absorbance increases. Furthermore, in the 2000–2008 cm<sup>-1</sup> region, a new transient absorption, whose position shifts slightly with alkane structure, grows in with an observed rate constant matching the rate of decay at 1947 cm<sup>-1</sup>. On the basis of kinetic analysis and literature precedent this new transient absorption has been assigned to the Rh alkyl hydride **4**, Cp\*Rh(CO)(H)(alkyl).<sup>23</sup>

We have found that these observations are general for each alkane studied except methane; we did not observe any reaction of **1** with methane in liquid Kr/CH<sub>4</sub> mixtures, even at methane concentrations in excess of 3 M.<sup>32</sup> Table 1 lists the IR absorptions assigned to the Rh alkyl hydride products for reaction of **1** with cyclohexane<sup>23</sup> and with the linear and cyclic<sup>33</sup> alkanes examined in the present study.

(28) For another example of temperature-dependent alkane IR band intensities, see: Snyder, R. G.; Maroncelli, M.; Strauss, H. L.; Hallmark, V. M. *J. Phys. Chem.* **1986**, *90*, 5623.

(29) For a thermodynamic study of binary ethane/Kr mixtures, see: Calado, J. C. G.; Chang, E.; Clancy, P.; Street, W. B. *J. Chem. Phys.* **1987**, *91*, 3914.

(30) Gomes de Azevedo, E. J. S.; Calado, J. C. G. *Fluid Phase Equilib.* **1991**, *90*, 215.

(31) Literature values for liquid Kr densities support a 17% density increase from –80 to –110 °C at the pressures pertaining in our experiments: Street, W. B.; Staveley, L. A. K. *J. Chem. Phys.* **1971**, *55*, 2495.

(32) At higher concentrations of methane, the solution became opaque in the IR region of interest, precluding a spectroscopic study.

(33) Kinetic studies with cyclopropane and cyclobutane as substrates were not undertaken because of potential complications arising from the observation of C–C activation of these strained rings by a related rhodium complex. See: Periana, R. A.; Bergman, R. G. *J. Am. Chem. Soc.* **1986**, *108*, 7346.

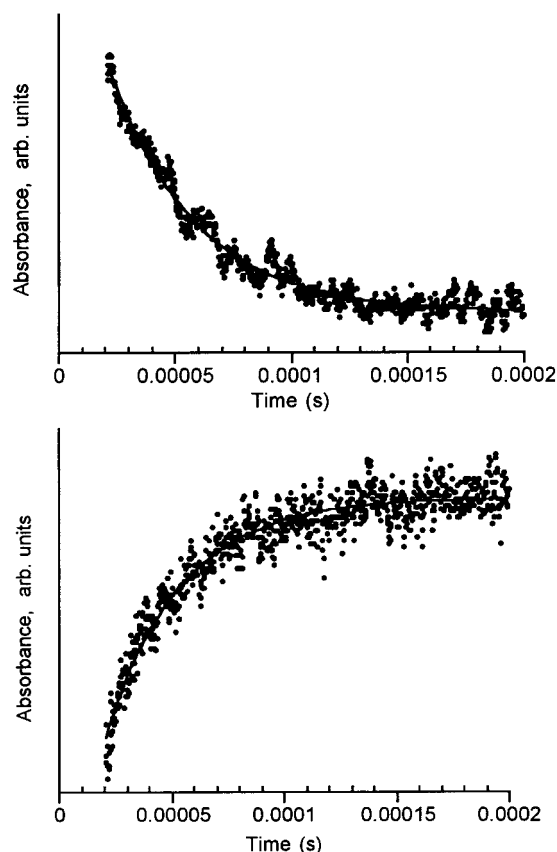


**Figure 1.** Representative kinetic traces for reaction of **1** in the presence of 1.7 mM octane in liquid Kr at –90 °C. The top trace shows decay of the absorbance at 1947 cm<sup>-1</sup>, due to disappearance of the Cp\*Rh(CO)•octane and Cp\*Rh(CO)•Kr adducts. The solid line is an exponential fit giving a  $k_{\text{obs}}$  value of  $2.7 \times 10^4 \text{ s}^{-1}$ . The bottom trace shows concurrent growth of the absorbance at 2005 cm<sup>-1</sup>, due to formation of Cp\*Rh(CO)(octyl)(H). The solid line is an exponential fit giving a  $k_{\text{obs}}$  value of  $3.0 \times 10^4 \text{ s}^{-1}$ .

Rates for the above reactions were measured under flooding conditions with submillimolar concentrations of **1** and alkane concentrations systematically varied in the 0.001–2 M range. Studies were carried out in the temperature range from –80 to –110 °C. Transient absorption traces at 1947 cm<sup>-1</sup> and in the 2000 cm<sup>-1</sup> region displayed pseudo-first-order behavior. Representative traces are illustrated in Figure 1. Overall rate constants,  $k_{\text{obs}}$ , were obtained by single-exponential fits to such traces. The  $k_{\text{obs}}$  values were then plotted against alkane concentration and the resulting curves fit according to the expression in eq 1 by nonlinear least-squares methods to afford values for  $k_2$  and  $K_{\text{eq}}$  at each temperature.<sup>34</sup> Figure 2 shows plots of  $k_{\text{obs}}$  vs alkane concentration for the series of linear hydrocarbons at –90 °C.

A clear trend correlating saturation behavior with alkane size is apparent. With ethane as substrate, the reaction rate does not begin to reach saturation until the alkane concentration exceeds 0.5 M. In contrast, the larger alkanes induce rate saturation at much lower concentration, indicative of larger  $K_{\text{eq}}$  values. Under the reaction conditions, rate saturation occurs because krypton no longer competes effectively with the alkane for coordination to the rhodium fragment in the preequilibrium. At this point  $k_{\text{obs}}$  may be equated with the rate constant for oxidative addition,  $k_2$ . Figure 3 shows a similar plot for reaction of the series of cyclic alkanes at –90 °C. The cyclohexane data from ref 23

(34) Curve fitting was performed using the commercially available program KaleidaGraph (Version 3.0, Synergy Software © 1996).

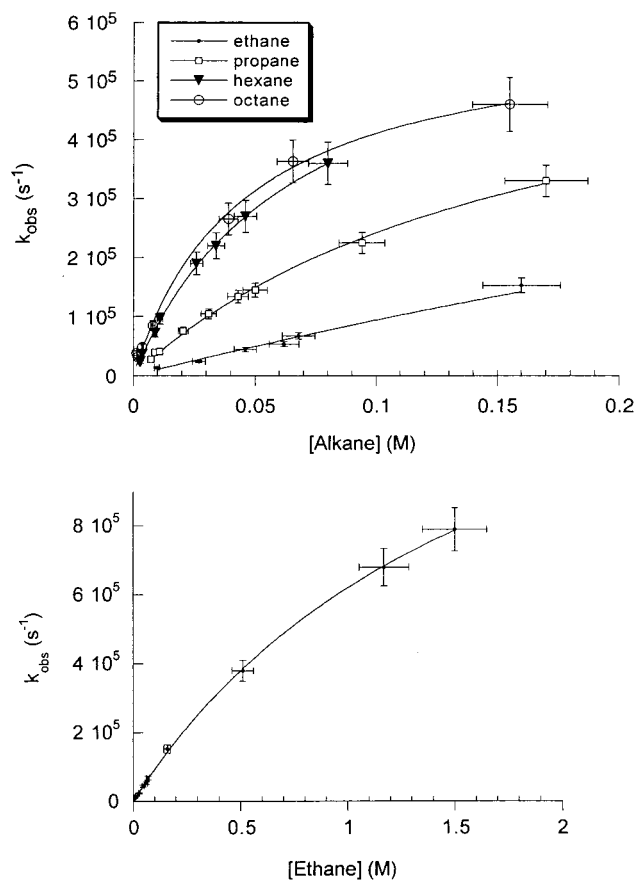


**Figure 2.** Plots of  $k_{\text{obs}}$  vs concentration of linear alkanes (top) and  $k_{\text{obs}}$  vs concentration of ethane over a larger concentration range (bottom) in liquid Kr at  $-90\text{ }^{\circ}\text{C}$ . The solid lines represent nonlinear least-squares fits of the data to eq 1.

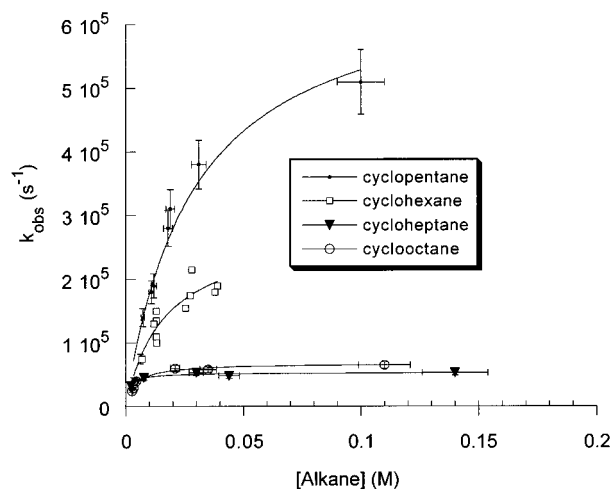


**Figure 3.** Plots of  $k_{\text{obs}}$  vs concentration of cyclic alkanes in liquid Kr at  $-90\text{ }^{\circ}\text{C}$ . The solid lines represent nonlinear least-squares fits of the data to eq 1.

have been reproduced for comparison with the data obtained in the present study. Here the impact of alkane size on the pre-equilibrium emerges even more dramatically, as the cycloheptane and cyclooctane reactions evidence rate saturation at close to the lowest alkane concentrations employed. A countervailing trend is evident in the rate of the insertion step characterized by  $k_2$ , which is highest for ethane, lowest for cyclooctane.

Table 2 shows the  $K_{\text{eq}}$  and  $k_2$  values extracted from plots such as those in Figures 2–3. Eyring plots of the temperature dependence of  $k_2$  (Figure 4) afford activation parameters for

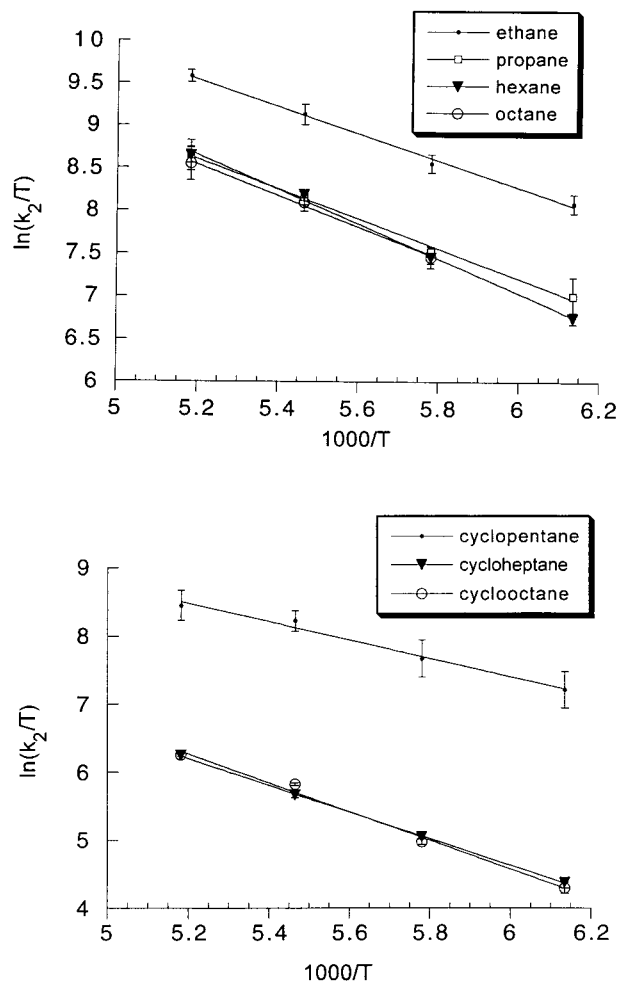
**Table 2.** Equilibrium and Rate Constants for Reaction of Alkanes with **1** in Liquid Kr<sup>a</sup>

alkane	$K_{\text{eq}}$	$k_2$ ( $10^5\text{ s}^{-1}$ )	
		$-80\text{ }^{\circ}\text{C}$	$-90\text{ }^{\circ}\text{C}$
ethane	$14 \pm 1$	$28 \pm 2$	$13 \pm 1$
propane	$140 \pm 10$	$11 \pm 1$	$140 \pm 10$
hexane	$350 \pm 50$	$11 \pm 2$	$340 \pm 20$
octane	$400 \pm 100$	$10 \pm 1$	$500 \pm 100$
cyclopentane	$1200 \pm 300$	$8.5 \pm 1$	$800 \pm 100$
cyclohexane <sup>b</sup>	$900 \pm 200$	$7.0 \pm 0.8$	$1500 \pm 300$
cycloheptane	$12000 \pm 2000$	$1.0 \pm 0.06$	$15000 \pm 3000$
cyclooctane	$15000 \pm 1000$	$1.0 \pm 0.02$	$15000 \pm 1000$

alkane	$K_{\text{eq}}$	$k_2$ ( $10^5\text{ s}^{-1}$ )	
		$-100\text{ }^{\circ}\text{C}$	$-110\text{ }^{\circ}\text{C}$
ethane	$12 \pm 1$	$9 \pm 1$	$11 \pm 1$
propane	$120 \pm 10$	$3.2 \pm 0.2$	$120 \pm 20$
hexane	$330 \pm 20$	$3.0 \pm 0.2$	$320 \pm 30$
octane	$600 \pm 100$	$3.0 \pm 0.2$	<i>d</i>
cyclopentane	$900 \pm 250$	$3.7 \pm 1$	$800 \pm 200$
cyclohexane	$2000 \pm 500$	$1.2 \pm 0.1$	$1500 \pm 300$
cycloheptane	<i>c</i>	$0.27 \pm 0.01$	<i>c</i>
cyclooctane	$14000 \pm 1000$	$0.25 \pm 0.01$	$13000 \pm 2000$

<sup>a</sup> Errors represent  $\pm\sigma$ . <sup>b</sup> Reference 23. <sup>c</sup> Saturation occurred at such low cycloheptane concentration that the data at these temperatures did not afford accurate  $K_{\text{eq}}$  values. <sup>d</sup> Octane was insufficiently soluble in Kr at  $-110\text{ }^{\circ}\text{C}$  to permit kinetic measurements.

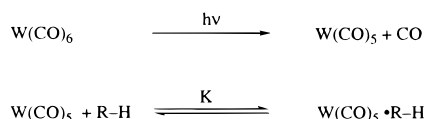


**Figure 4.** Eyring plots of the temperature dependence of  $k_2$  values for the oxidative addition of linear alkanes (top) and cyclic alkanes (bottom) to the  $\text{Cp}^*\text{Rh}(\text{CO})$  fragment in the temperature range from  $-80$  to  $-110\text{ }^{\circ}\text{C}$ .

the oxidative addition step; these are summarized in Table 3. The errors in  $K_{\text{eq}}$  values are sufficiently large relative to the variation of these values with temperature that we felt a rigorous

**Table 3.** Activation Parameters for  $k_2$ , Oxidative Addition of Alkanes to the Cp\*Rh(CO) Fragment<sup>a</sup>

alkane	$\Delta H^\ddagger$ (kcal/mol)	$\Delta S^\ddagger$ (cal/mol•K)
ethane	3.6 ± 0.4	-9 ± 3
propane	3.9 ± 0.4	-10 ± 2
hexane	4.6 ± 0.6	-8 ± 3
octane	3.6 ± 1	-11 ± 6
cyclopentane	2.7 ± 1	-16 ± 5
cyclohexane <sup>b</sup>	4.6 ± 0.6	-7 ± 6
cycloheptane	3.9 ± 0.4	-12 ± 2
cyclooctane	4.6 ± 0.4	-11 ± 2

<sup>a</sup> Errors represent ± $\sigma$ . <sup>b</sup> Reference 23.**Scheme 2**

van't Hoff treatment was not warranted. We note only that for every alkane studied, van't Hoff analysis yields a *positive* entropy change in the direction of the alkane complex, with values ranging from approximately 5 to 20 eu.

**Photolysis of 1 in Liquid Xenon/Alkane Solutions.** As shown previously in our group, photolysis of **1** in pure liquid xenon produces a transient species absorbing at 1941 cm<sup>-1</sup>. At -80 °C this transient is longer lived than the analogous Kr species and has been assigned to the xenon solvate, Cp\*Rh(CO)•Xe.<sup>23</sup> We have observed in the present study that photolysis of **1** in mixtures of xenon/methane, xenon/ethane, or xenon/propane results only in observation of the single transient band at 1941 cm<sup>-1</sup>. Moreover, the decay of this absorbance appears to remain unchanged from that in pure liquid Xe, even at relatively high concentrations of alkane. In contrast, upon photolysis of **1** in Xe solutions containing butane and larger alkanes, rates of decay of the 1941 cm<sup>-1</sup> absorption increase with increasing alkane concentration. Furthermore, absorption by an alkyl hydride product, Cp\*Rh(CO)(alkyl)(H), is observed in the 2000 cm<sup>-1</sup> region. Kinetic data for the reaction of **1** with cyclohexane in liquid Xe were published in an earlier study.<sup>23</sup>

**Discussion****Trends in the Preequilibrium Binding of Alkanes to Rh.**

The data reported here supplement our earlier studies, in which rates were measured for the photoinduced reaction of **1** in rare gas solutions of cyclohexane and neopentane. When the data are considered as a whole, the clearest trend that emerges is a shift in the preequilibrium from the krypton complex toward the alkane complex as alkane size increases. This effect is preceded in a study by Rayner, Hackett, and co-workers on alkane binding affinities toward photogenerated W(CO)<sub>5</sub> in the gas phase.<sup>35</sup> In contrast to the rhodium system studied here, the electronically unsaturated tungsten complex does not induce oxidative addition of C–H bonds, but rather forms transiently stable alkane adducts of the type postulated in the rhodium preequilibrium (Scheme 2). The study demonstrated that the equilibrium between naked W(CO)<sub>5</sub> and W(CO)<sub>5</sub>(alkane) shifts toward the alkane complex as alkane size increases. The hydrocarbons in that study ranged in size from methane to hexane and cyclohexane, and the magnitudes of increase in the observed equilibrium constants match those in the present study reasonably well. Significantly, methane appeared not to bind

(35) Brown, C. E.; Ishikawa, Y.; Hackett, P. A.; Rayner, D. M. *J. Am. Chem. Soc.* **1990**, *112*, 2530.**Table 4.** Rare Gas and Alkane Ionization Potentials and Polarizabilities and Free Energies for the Kr/Alkane Complex Equilibria at -90 °C

substrate	first IP (eV)	polarizability <sup>e</sup> (Å <sup>3</sup> )	$\Delta G_{183K}$ (kcal/mol)
Kr	14.00 <sup>a</sup>	2.74	
Xe	12.13 <sup>a</sup>	4.46	
methane	12.75 <sup>b</sup>	2.61	>0
ethane	11.56 <sup>b</sup>	4.5	-0.9
propane	10.9 <sup>b</sup>	6.36	-1.8
hexane	9.97 <sup>c</sup>	11.9	-2.1
octane	9.71 <sup>d</sup>	15.6	-2.3
cyclopentane	10.33 <sup>d</sup>	9.11	-2.4
cyclohexane	9.82 <sup>c</sup>	10.96	-2.6
cycloheptane	9.96 <sup>c</sup>	12.1	-3.5
cyclooctane	9.75 <sup>c</sup>	13.9	-3.5

<sup>a</sup> Reference 36. <sup>b</sup> Reference 37. <sup>c</sup> Reference 38. <sup>d</sup> Reference 39. <sup>e</sup> Reference 43.

to the tungsten species at all, consistent with our failure to observe any interaction between methane and the Rh–Kr solvate.

The authors of the tungsten study attribute the size effect to improved orbital interaction between the LUMO on tungsten and the C–H  $\sigma$  molecular orbital on the alkane. They argue that as alkane size increases, so, too, does the energy of the C–H  $\sigma$  MO (as determined by photoelectron spectroscopy), and as the energy gap shrinks between this orbital and the tungsten LUMO, the interaction becomes more favorable. Table 4 lists the first ionization potentials for each alkane considered in the present study.<sup>36–39</sup> The values decrease with increasing alkane size, indicative of rising orbital energies.

The above argument is consistent with treating the metal–alkane interaction as fundamentally “soft”, in accordance with hard/soft acid base principles.<sup>40,41</sup> The small (or nonexistent) dipole moments, low basicities, and high ionization potentials associated with alkanes and the larger noble gases argue for the importance of an induced distortion of electron clouds in the bonding between these weak ligands and transition metal centers.<sup>42</sup> Binding affinities should then correlate with polarizabilities. As the polarizability of the ligand increases, so, too, should the strength of interaction between that ligand and the soft metal center. The polarizabilities of Kr, Xe, and the alkanes employed as substrates are also listed in Table 4, accompanied by the free energies characterizing the preequilibria at -90 °C.<sup>43</sup> It is particularly noteworthy that Kr and methane have comparable polarizabilities, as do Xe, ethane, and propane. These numbers support the hypothesis that coordinative competition between hydrocarbons and rare gas atoms for the unsaturated rhodium center is influenced by the relative polarizabilities of these ligands. Thus methane does not effectively compete with the equally polarizable Kr, given that the Kr is present in 10- to 1000-fold excess, and similarly ethane and propane compete

(36) Kimura, K.; Katsumata, S.; Achiba, Y.; Yamazaki, T.; Iwata, S. Ionization energies, ab initio assignments, and valence electronic structure for 200 molecules. In *Handbook of HeI Photoelectron Spectra of Fundamental Organic Compounds*; Japan Scientific Society Press: Tokyo, 1981.(37) Bieri, G.; Burger, F.; Heilbronner, E.; Maier, J. P. *Helv. Chim. Acta* **1977**, *60*, 2213.(38) Sieck, L. W.; Mautner (Meot-Ner), M. *J. Phys. Chem.* **1982**, *86*, 3646.(39) Mautner (Meot-Ner), M.; Sieck, L. W.; Ausloos, P. *J. Am. Chem. Soc.* **1981**, *103*, 5342.(40) Parr, R. G.; Pearson, R. G. *J. Am. Chem. Soc.* **1983**, *105*, 7512.(41) Pearson, R. G. *J. Am. Chem. Soc.* **1988**, *110*, 7684.(42) For a theoretical treatment of the bonding in transition metal rare gas complexes, see: Ehlers, A. W.; Frenking, G.; Baerends, E. J. *Organometallics* **1997**, *16*, 4896.(43) Applquist, J. *J. Phys. Chem.* **1993**, *97*, 6016 and references therein.

poorly with excess Xe. In contrast, the larger, softer, more polarizable alkanes interact more strongly with the unsaturated Rh center than do the rare gas atoms, and thus the equilibria are driven toward the alkane complexes.

For propane, hexane, and octane, binding affinities seem to correlate reasonably well with polarizability. However, the cyclic alkanes uniformly exhibit higher  $K_{\text{eq}}$  values than their linear counterparts, despite comparable polarizabilities. Furthermore, the increase in polarizability with carbon number is roughly constant, whereas the data evidence a large discontinuity in the relative  $K_{\text{eq}}$  values between cyclopentane and cyclooctane. Clearly a second physical phenomenon (or phenomena) augments polarizability in determining the binding energetics of cyclic substrates.

It is likely that subtle steric and conformational factors influence the particularly strong affinity of the Rh center toward the seven- and eight-membered rings. van der Waals attractions between the Rh fragment and distant sites on these larger hydrocarbons may be significant in this regard. Solvent effects may also play a strong role in the equilibrium between the Kr and alkane complexes. In fact it is plausible that our measured binding energies, to a large extent, simply reflect differential solvation of the alkanes in krypton. From an entropic standpoint, binding of the alkane to the Rh center should liberate a number of krypton atoms associated with solvation of the free alkane. As alkane size increases, liberation of these Kr atoms should become increasingly entropically favorable, thus driving the equilibrium toward the metal-alkane complex. This argument is consistent with the positive entropy changes suggested by van't Hoff analysis. Changes in solvation enthalpies for the free alkanes and Rh-alkane complexes could contribute as well. Despite careful consideration of the data, however, a compelling physical model that accounts for all of the binding phenomena remains elusive.

**Rates of Oxidative Addition.** The dependence of the  $k_2$  values, reflecting elementary rates of C-H oxidative addition, on alkane structure is roughly opposite to that observed for the binding constants. Thus the ethane reaction is rapid, while longer linear alkanes react at similar, slower rates. Cyclic alkanes react more slowly than their linear counterparts, and the reactions of cycloheptane and cyclooctane are remarkably slow.<sup>44</sup>

It seems most straightforward to interpret this trend as a ground-state effect resulting from the same factors that influence binding in the preequilibrium. This is illustrated in Figure 5, which shows a proposed reaction coordinate diagram for the reactions of **1** with cyclopentane and with cyclooctane at  $-90$  °C. Cyclooctane's strong binding relative to cyclopentane places the Rh-C<sub>8</sub>H<sub>16</sub> complex 1.1 kcal/mol lower in energy than the Rh-C<sub>5</sub>H<sub>10</sub> complex. Whatever the cause of this strong binding, some of it seems to be lost in going from each alkane complex to the corresponding C-H activation transition state. That is, the free energy gap between alkane complexes ( $\Delta\Delta G$ ) is larger than the gap between transition states for oxidative addition ( $\Delta\Delta G^\ddagger$ ). Thus the transition states for oxidative addition of the different alkanes lie closer together in energy than do the respective precursor alkane complexes, and the rate of oxidative addition is therefore slowest for the most strongly bound alkanes. The logic of this argument suggests that oxidative addition of methane from the alkane complex may proceed with the smallest relative barrier. However, in contrast to the other alkane

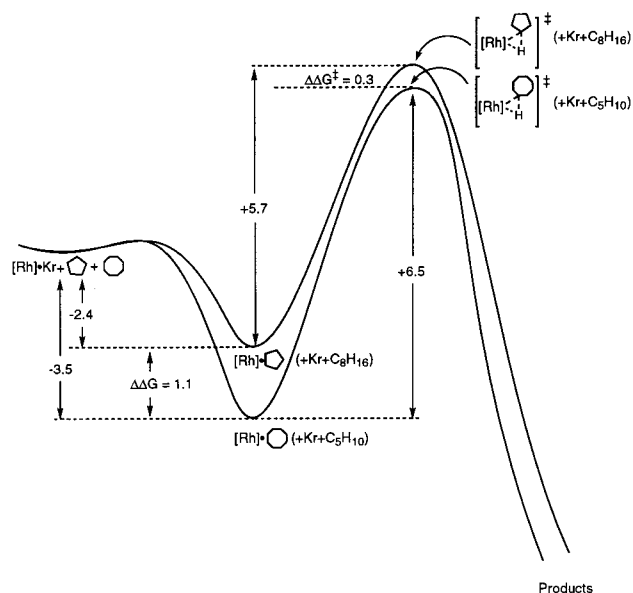


**Figure 5.** Reaction coordinates for reaction of **1** with cyclopentane and with cyclooctane in liquid Kr solution at  $-90$  °C. Free energies listed are in kcal/mol. [Rh] = Cp\*Rh(CO). The diagram is not drawn precisely to scale.

complexes, the Rh-CH<sub>4</sub> complex appears to lie higher in energy than the krypton complex; consequently it forms in such low abundance that reaction with methane is not observed.

Steric factors probably also play a role in determining relative oxidative addition rates. In the cyclic series, the transition states for formation of cycloheptyl and cyclooctyl Rh hydride species may be particularly conformationally demanding. Regarding the trend in the linear series, propane is more hindered than ethane, but the longer chain hydrocarbons may not suffer significantly more hindrance than propane, particularly if activation occurs predominantly at the terminal CH<sub>3</sub> groups. This reasoning is consistent with the similarity in rates for propane, hexane, and octane. Unfortunately, such a hypothesis is difficult to confirm, since the methodology employed in this study does not distinguish between activation at primary and secondary sites.<sup>45</sup>

It was hoped that Eyring analysis of the  $k_2$  data would give further insight into the trend in oxidative addition rates. However, an examination of the activation enthalpies and entropies in Table 3 reveals no obvious trend across the full series of hydrocarbons. It is worth noting that (1) a negative activation entropy is consistent with the stereoelectronic demands of oxidative addition and (2) the small activation enthalpies (ca. 4 kcal/mol) for the cleavage of such strong bonds support significant Rh-C and/or Rh-H interaction in the transition state.

## Conclusions

The kinetic data for the photoinduced reaction of Cp\*Rh(CO)<sub>2</sub> with linear and cyclic saturated hydrocarbons support a strong influence of alkane structure on the binding affinity of the alkane toward the unsaturated rhodium center in the Cp\*Rh(CO) fragment. In the initially formed alkane or  $\sigma$ -complex, larger alkanes interact more strongly with the Rh fragment than

(44) Compensating variations in the parameters of a dual parameter fit can sometimes simply be artifacts of the fitting equation. In this case, however, we directly observe saturation behavior, and we are therefore confident that physical phenomena differentiate the rates and equilibria in, for example, the cyclohexane and cycloheptane reactions.

(45) For the related Cp\*Rh(P(CH<sub>3</sub>)<sub>3</sub>) fragment, Periana and Bergman showed that activation of butane at  $-100$  °C produces only the primary (CH<sub>3</sub>-activated) rhodium butyl hydride, as evidenced by <sup>1</sup>H NMR. In that case, however, the observed product may have been thermodynamic, rather than kinetic: Periana, R. A.; Bergman, R. G. *J. Am. Chem. Soc.* **1986**, *108*, 7332.

do smaller alkanes. Methane does not appear to bind at all, while ethane binds an order of magnitude less strongly than the longer chain hydrocarbons. Cyclic alkanes appear to bind more favorably than comparably sized linear alkanes. Furthermore, there is a pronounced discrepancy between the binding energetics of cyclohexane and cycloheptane, which differ by an order of magnitude.

Elementary rates of C–H oxidative addition follow an opposing trend. Thus reaction of the Rh–ethane complex to form Cp\*Rh(CO)(ethyl)(H) is most rapid, while reaction of the cycloheptane and cyclooctane complexes is anomalously slow. It is likely that solvent effects in the noble gas media play a significant role in the above trends. Nonetheless, the results highlight the general importance of treating C–H bond activa-

tion at late metal centers as a two-step process, with potentially different factors influencing the binding step and activation step.

**Acknowledgment.** We are grateful to a reviewer of the manuscript for insights into interpretation of the trend in cyclic alkane binding affinities. This work was supported by the Director, Office of Energy Research, Office of Basic Energy Sciences, Chemical Sciences Division, U.S. Department of Energy, under contract No. DE-AC03-76SF00098.

**Supporting Information Available:** Derivation of the rate expression in eq 1 (PDF). This material is available free of charge via the Internet at <http://pubs.acs.org>.

JA9904282